JOURNAL OF MAGNETIC RESONANCE **132,** 130–137 (1998)
ARTICLE NO. MN981406

Detection of Nitrogen–Nitrogen *J*-Couplings in Proteins

Frank Löhr and Heinz Rüterjans[1]

Institut für Biophysikalische Chemie, Johann Wolfgang Goethe-Universität, Biozentrum N230, Marie Curie-Straβe 9, D-60439 Frankfurt am Main, Germany

E-mail: hruet@peter.bpc.uni-frankfurt.de

Received October 22, 1997; revised January 21, 1998

Methods are described which allow the measurement of geminal and vicinal $^{15}N-^{15}N$ coupling constants in isotopically labeled proteins. The experiments rely on a quantitative *J*-correlation strategy and include either N,N-COSY or N,N-TOCSY magnetization transfer steps. The pulse sequences are demonstrated with a 16-kDa protein. Although the $^{3}J_{NN}$ couplings are almost vanishingly small, they give rise to visible cross peaks for 56% of the amino acid residues. A dependence of the vicinal coupling constants on the backbone torsion angle ψ is observed. However, only in favorable cases can the ^{3}J values be translated into local structural information. In arginine side chains, correlations between ϵ- and η-nitrogens via two-bond scalar couplings are obtained that can be exploited for the resonance assignment of the guanidino groups.

Key Words: ***J*-coupling constants; quantitative *J*-correlation; ψ-torsion angle; resonance assignment; flavodoxin.**

INTRODUCTION

Scalar three-bond couplings are now commonly used in the structure determination of small and medium-sized proteins (*1, 2*). Experiments for the measurement of such coupling constants mainly provide information about the ϕ and χ^1 torsion angles. In contrast, constraints for the backbone torsion angle ψ—if included at all—were up to now mostly based on NOE intensities and the chemical shift index (*3*) and limited to regular secondary structure elements. Very recently, an elegant approach for this purpose has emerged which relies on cross-correlated dipole–dipole and dipole–CSA relaxation, respectively, to detect the relative orientations of either the $C^{\alpha}-H_i$ and $N-H_{i+1}$ bond vectors (*4*) or the $C^{\alpha}-H_i$ bond vector and the C'_i CSA tensor (*5*). A correlation between the backbone geometry and one-bond (*6*) as well as two- and three-bond (*7*) deuterium isotope shifts on $^{13}C^{\alpha}$ chemical shifts is also evident.

Interresidual $^{1}H^{\alpha}-^{15}N$ ^{3}J coupling constants can readily be measured in isotopically labeled proteins using E.COSY-type techniques (*8–10*), and their dependence on the ψ-angle has been empirically established (*10*). Because of the inherent degeneracy of the Karplus relationship (*11*), it is, however, desirable to obtain additional ψ-related dihedral angle information. The magnitude of five-bond $^{1}H^{\alpha}-^{1}H^{\alpha}$ couplings between adjacent amino acid residues in small peptides has been shown to depend on the configuration of the peptide bond and the intervening ϕ and ψ torsion angles (*12–14*). Therefore, it was suggested to exploit this long-range interaction to limit the ψ-conformational space once the ϕ-angle has been determined independently (*15*). Similarly, $^{1}J(C^{\alpha},N)$, $^{2}J(C^{\alpha},N)$, $^{1}J(C^{\alpha},H^{\alpha})$, and $^{2}J(C',H^{\alpha})$ coupling constants, which are readily accessible in $^{13}C/^{15}N$ enriched proteins, exhibit a clear dependence on the position in the $\phi-\psi$ space (*16–19*) and are therefore indicative of the secondary structure, but their translation into ψ-constraints may not be straightforward. A more direct dependence on the ψ-angle can be expected for the vicinal coupling between adjacent backbone ^{15}N nuclei. However, this type of homonuclear interaction has to the best of our knowledge never been observed in proteins, probably because of its very small magnitude. Nevertheless, it is attempted in the present study to determine the coupling quantitatively and to assess whether it possibly contains useful structural information.

RESULTS AND DISCUSSION

The quantitative *J*-correlation approach has been proven to be a reliable means for the measurement of homonuclear coupling constants (*2*). The pulse schemes employed here are closely related to methods proposed for the determination of $^{13}C',^{13}C'$ *J*-couplings (*20, 21*). In the HNN experiment depicted in Fig. 1A, amide proton ($^{1}H^{N}_{i}$) magnetization is first transferred to the directly bound ^{15}N nucleus. During the subsequent delay δ antiphase ^{15}N coherence can build up with respect to any long-range coupled nitrogen spin, allowing a COSY-type transfer by the 90° pulse of phase ψ_3. Following the t_1 period in which $^{15}N_i$ and $^{15}N_{i\pm1}$ chemical shifts evolve, the magnetization is transferred back for

[1] To whom correspondence should be addressed. Fax: +49-69-798-29632.

1090-7807/98 $25.00

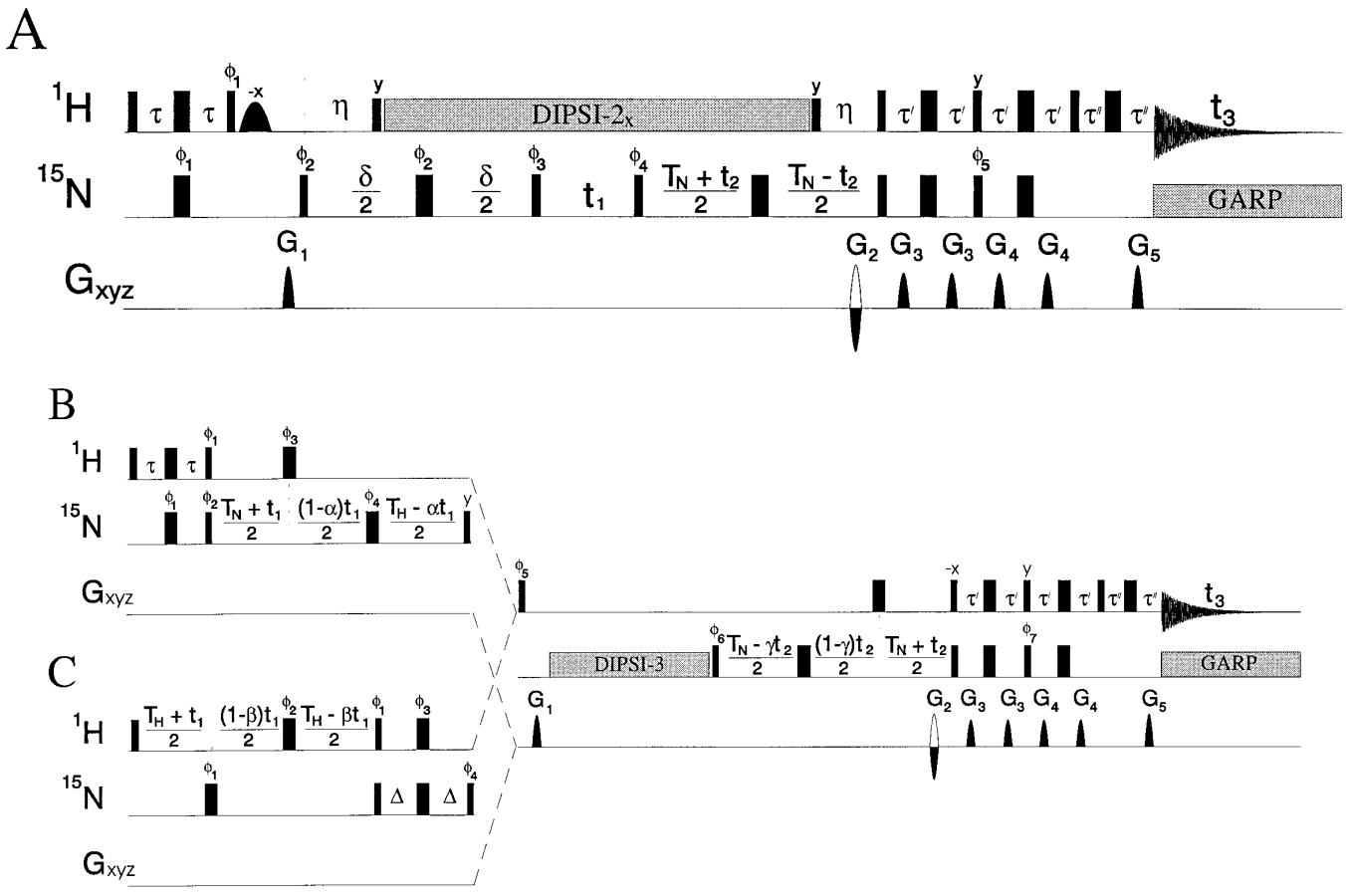

FIG. 1. Pulse schemes for the quantitative ^{15}N,^{15}N correlation: (A) the HNN experiment, (B) (H)NNH and (C) H(N)NH versions of the HNNH-TOCSY experiment. Narrow and wide bars represent hard 90° and 180° rectangular pulses, respectively. The nitrogen carrier frequency is placed in the center of the amide region (118.7 ppm), and the proton carrier is set to the H_2O resonance frequency (4.75 ppm) throughout sequences B and C while it is temporarily switched to 6.71 ppm for the application of the DIPSI-2 (*22*) decoupling sequence (4.5-kHz RF field) in A. The water-selective pulse in the HNN experiment is Gaussian-shaped and has a duration of 2.5 ms corresponding to a flip angle of 90°. Isotropic mixing in the HNNH-TOCSY experiments is achieved with the DIPSI-3 (*22*) sequence at an RF field strength of 1.5 kHz. GARP-1 (*23*) modulation (0.75 kHz) is used for ^{15}N decoupling during acquisition. Fixed delays are set as follows: (A) τ = 2.3 ms, η = 5.4 ms, τ' = 2.5 ms, τ'' = 0.7 ms; (B, C) τ = 2.3 ms, $T_H = T_N$ = 5.4 ms, Δ = 2.7 ms, τ' = 2.5 ms, τ'' = 0.7 ms. Values for δ and T_N in the HNN experiment are either 120 or 150 ms. The factors α, β, and γ in the semiconstant time evolution periods of the HNNH-TOCSY experiments are adjusted to 0.075, 0.189, and 0.147, respectively. Sine-bell-shaped gradients have the following durations and approximate strengths at their center: G_1: 1 ms, 5 G cm^{-1} (y); G_2: 1 ms, −39.5/39.5 G cm^{-1} (z); G_3: 0.5 ms, 4 G cm^{-1} (x), 5.5 G cm^{-1} (y); G_4: 0.5 ms, 5.5 G cm^{-1} (x), 4 G cm^{-1} (y); G_5: 0.5 ms, 8 G cm^{-1} (z). For each t_2 increment N- and P-type signals are collected alternately by inverting the polarity of G_2 along with the pulse phases ϕ_5 (A) or ϕ_7 (B, C). In HNNH-TOCSY experiments, the phase ϕ_6 is inverted along with the receiver reference phase in every other t_2 increment. The States-TPPI method (*24*) is applied to phases ϕ_2 and ϕ_3 in sequence A and to phase ϕ_2 in sequence B to achieve quadrature detection in t_1. Phase cycles are (A) $\phi_1 = y,-y$; $\phi_2 = 2(x),2(-x)$, $\phi_3 = 4(x),4(-x)$; $\phi_4 = 8(x),8(-x)$; rec. = $x,2(-x),x$; (B) $\phi_1 = y,-y$; $\phi_2 = x$; $\phi_3 = 2(x),2(y)$; $\phi_4 = 2(x),2(-x),2(y),2(-y)$; $\phi_5 = 2(-x),2(x)$; $\phi_6 = 2(y),2(-y)$; $\phi_7 = y$; rec. = $x,2(-x),x,-x,2(x),-x$; and (C) $\phi_1 = y,-y$; $\phi_2 = 4(x),4(-x)$; $\phi_3 = 2(x),2(y)$; $\phi_4 = 4(y),4(-y)$; $\phi_5 = 2(-x),(x)$; $\phi_6 = 2(y),2(-y)$; $\phi_7 = y$; rec. = $x,2(-x),x,-x,2(x),-x$. Nonlabeled pulses are applied along the x-axis.

$^1H^N_i$ detection along the reverse pathway. The rephasing period T_N is exploited for constant time ^{15}N (t_2) evolution in order to disperse the signals along a third dimension. It should be noted, however, that an improved resolution is only achieved for cross peaks ($^{15}N_{i\pm1}$, $^{15}N_i$, $^1H^N_i$), but not for diagonal peaks, where two of the three chemical shifts are identical. Gradient pathway selection combined with sensitivity enhancement is employed in the final reverse INEPT step (*25, 26*). In order to avoid a saturation of fast-exchanging amide protons the water magnetization is kept along the z-axis during the application of gradient pulses G_1, G_2, and G_5 using an H_2O selective flip-back pulse (*27*) and temporarily aligned with the spin-lock axis of the DIPSI-2 decoupling sequence such that no dephasing due to RF inhomogeneity occurs (*28*). A similar pulse sequence has been used for the measurement of $^2J_{NN}$ coupling constants in an organometallic complex (*29*). The fraction of the source-^{15}N magnetization that is transferred to a coupled ^{15}N nucleus depends on the size of the coupling constant and the length of the dephasing and rephasing periods. The ^{15}N–^{15}N coupling constants

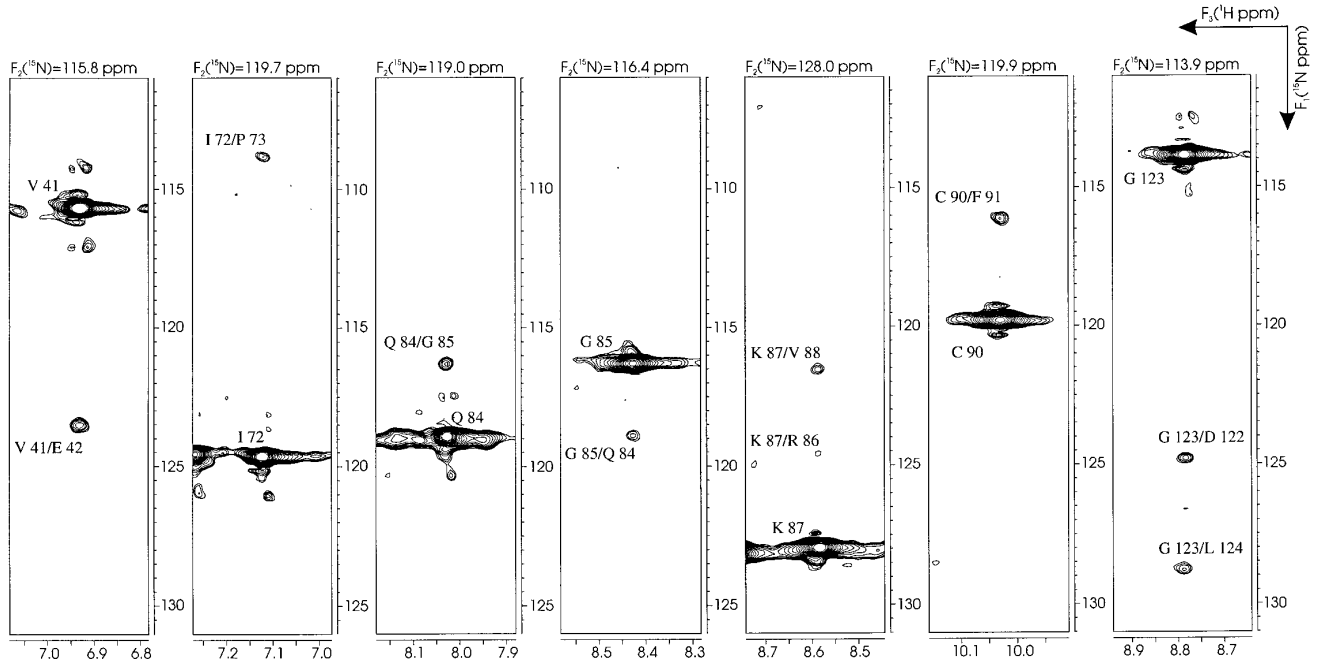

FIG. 2. Selected F_1-F_3 strips from a 600-MHz 3D HNN spectrum (δ = 150 ms) of *D. vulgaris* flavodoxin. The positions of the slices in F_2 are indicated at the top of each panel. Diagonal and cross peaks have opposite intensities. Positive and negative contours are plotted without distinction. The level spacing factor is uniformly set to $2^{1/3}$. The I 72/P 73 cross peak is aliased in the F_1 dimension and corresponds to a ^{15}N chemical shift of 135.6 ppm. The following $^3J_{NN}$ coupling constants were calculated from the relative peak intensities: V 41/E 42: 0.28 Hz, I 72/P 73: 0.21 Hz, Q 84/G 85: 0.29 Hz, K 87/R 86: 0.14 Hz, K 87/V 88: 0.22 Hz, C 90/F 91: 0.29 Hz, G 123/D 122: 0.29 Hz and G 123/L 124: 0.31 Hz.

can therefore be calculated from the relative volume integrals of cross peaks (V_C) and diagonal peaks (V_D) according to $V_C/V_D = -\tan^2(\pi J_{NN}\delta)$ (*30*). As the lineshapes of cross peaks and diagonal peaks are identical in F_2 and F_3 and vary significantly in F_1 only in the case of substantially different transverse relaxation rates of two neighboring ^{15}N nuclei, backbone $^3J_{NN}$ couplings can be determined to a very good approximation from the ratio of peak heights instead.

The quantitative ^{15}N,^{15}N *J*-correlation was applied to oxidized *Desulfovibrio vulgaris* flavodoxin, which consists of 147 amino acid residues and a very tightly, noncovalently bound flavin mononucleotide cofactor. Two HNN spectra, recorded with $T_N = \delta = 120$ ms and $T_N = \delta = 150$ ms, yielded a total of 53 vicinal ^{15}N–^{15}N coupling constants ranging from 0.13 to 0.32 Hz. In Fig. 2, several examples from the data set recorded with dephasing and rephasing periods of 150 ms are shown. The lower limit of the $^3J_{NN}$ values that can be measured depends on the signal-to-noise ratio of the cross peaks, which is to a large extent governed by the transverse relaxation times of the amide nitrogens. An average T_2 value of approximately 140 ms was found for *D. vulgaris* flavodoxin in the oxidized state (*31*). For about 10% of the residues, coupling constants could not be obtained reliably either because of resonance overlap of two diagonal peaks or because cross peaks resonating within ±2 ppm of the nitrogen chemical shift of the diagonal peak could not be identified unambiguously. In many cases $^3J_{N(i)N(i+1)}$ couplings were determined twice in the same spectrum (e.g., Q 84/G 85 in Fig. 2) since the magnetization transfer occurs from N(i) to N(i + 1) and vice versa, leading to an improved reliability. Differential relaxation of ^{15}N in-phase and antiphase magnetization may cause a decrease of the apparent coupling constants, considering that the lengths of dephasing and rephasing periods employed here are a considerable fraction of the average ^{15}N T_1 time of about 500 ms (*31*). Because these periods are short compared to $1/(2^3J_{NN})$, though, the systematic error can be calculated in the same way as for the measurement of $^3J_{H^N H^\alpha}$ in the HNHA experiment (*32*). The underestimation of the $^3J_{NN}$ couplings in the HNN experiment due to ^{15}N spin flips accordingly amounts to 11% for δ = 120 ms and 13.5% for δ = 150 ms. Experimentally, a trend toward lower values at longer dephasing and rephasing periods was not observed and the coupling constants reported here are not corrected for this effect. The rms pairwise difference between the measurements with δ = 120 ms and δ = 150 ms was 0.04 Hz.

Apart from the backbone, potential ^{15}N,^{15}N scalar interactions in proteins can be expected in arginine side chains. The corresponding $^{15}N^{\eta}$,$^{15}N^{\epsilon}$,$^1H^{N\epsilon}$ (F_1, F_2, F_3) cross peaks were observed in the HNN spectra for six of the seven arginine residues in flavodoxin. Complementary correlations (i.e., those originating from $^1H^{N\eta}$) cannot be detected because the choice of a delay duration of $\eta = 1/(2J_{NH})$ in the pulse sequence of Fig. 1A results exclusively in coherences

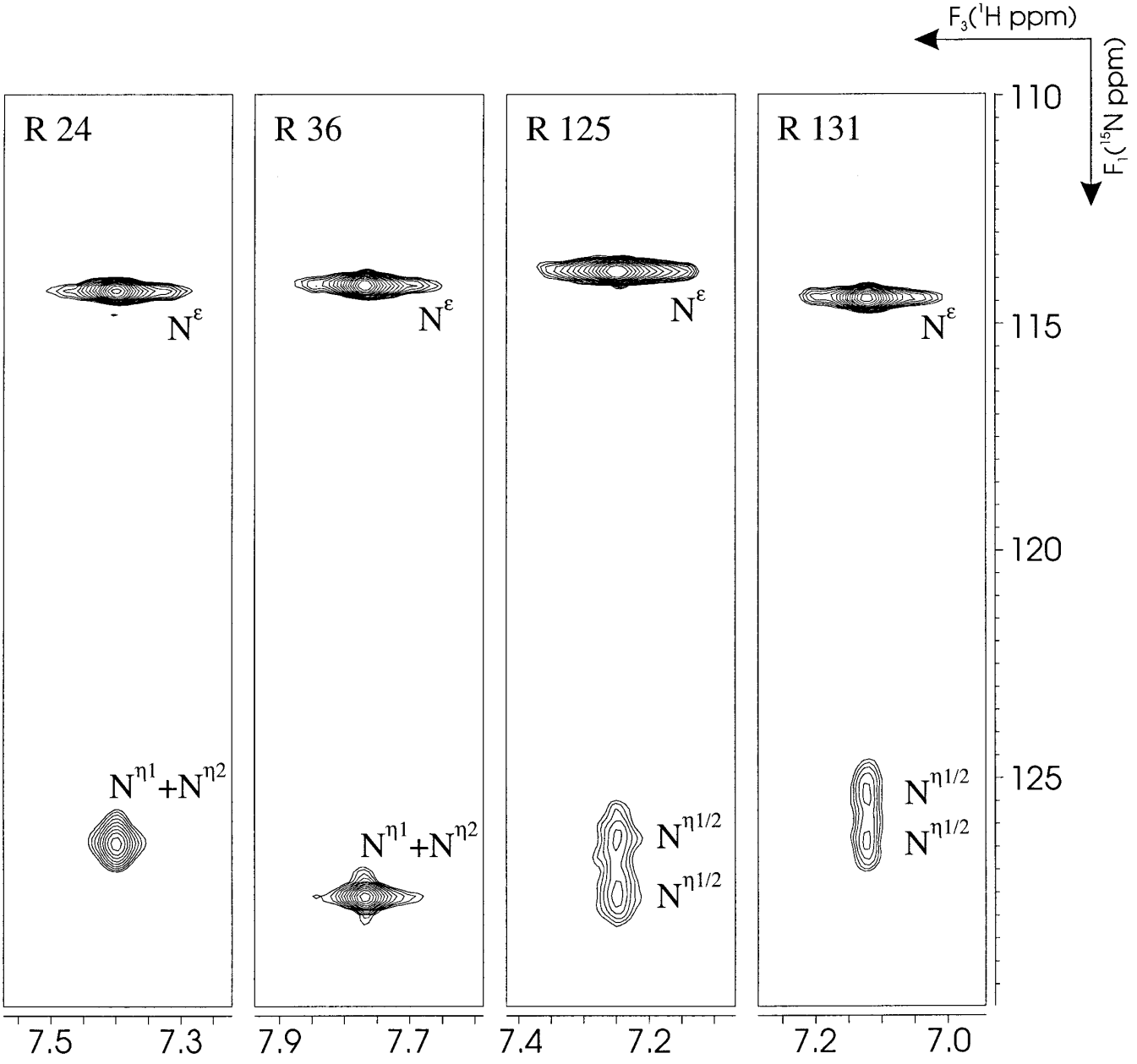

FIG. 3. Expansions from HNN F_1-F_3 slices taken at the $^{15}N^{\epsilon}$ (F_2) chemical shifts of arginine residues in flavodoxin. In F_1, N^{ϵ} diagonal peaks are folded once and N^{η} peaks are folded twice so that their real positions are 26.7 and 53.4 ppm, respectively, upfield from the values directly read from the scale. The labels $\eta 1/2$ indicate that no individual assignments for the guanidino NH_2 groups are available.

that are not converted into observable magnetization in NH_2 groups. Furthermore, the latter pathway would be strongly attenuated by the line broadening of η proton and nitrogen resonances caused by chemical exchange processes. As shown in Fig. 3, either one or two cross peaks are obtained for the two η-nitrogens in the HNN experiment, reflecting different rates of the rotation about the $N^{\epsilon}-C^{\zeta}$ bond, unless their chemical shifts are accidentally degenerate. Among the six arginine side chains the magnitude of the $^2J_{N\epsilon N\nu}$ couplings through which the magnetization transfer takes place varied between 0.9 and 1.1 Hz. For their quantitative measurement, volume integrals rather than peak heights were determined because of the clearly unequal linewidths of diagonal and cross peaks. Although the knowledge of the size of these two-bond coupling constants appears not to be relevant, their mere existence might be exploited to assign the η-nitrogen resonances of the guanidino moieties by a correlation to the more readily accessible $^{15}N^{\epsilon}$ chemical shifts.

As mentioned earlier, the most critical limitation of a quantitative $^{15}N,^{15}N$ J-correlation is its low sensitivity. Re-

cently it has been demonstrated in the context of the $^3J_{C'C'}$ determination that a more efficient homonuclear magnetization transfer is achieved when the pulse-interrupted free precession period is replaced by an isotropic mixing sequence (*21*). This either allows the measurement of yet smaller coupling constants or makes the method feasible for proteins with less favorable relaxation properties. The HNNH-TOCSY experiment (Figs. 1B, C) represents an adaptation of the (HN)CO(CO)NH scheme (*21*) to the measurement of $^3J_{NN}$. Following the initial refocused INEPT step, in-phase ^{15}N magnetization is rotated to the *z*-axis and subsequently exposed to a DIPSI-3 mixing period where a net polarization transfer to the amide nitrogen of an adjacent amino acid residue can take place. Frequency labeling of the destination ^{15}N spin is achieved during t_2 in a semiconstant-time manner (*33, 34*) just before the gradient-selected sensitivity-enhanced magnetization transfer to the directly bound protons. The 90° proton pulse of phase ϕ_5 applied prior to the start of the isotropic mixing sequence requires some explanation, as it serves two different purposes. It acts as a purge pulse to destroy N_yH_z antiphase terms of asparagine and glutamine NH_2 groups through its phase cycle in combination with the gradient G_1. At the same time water magnetization which originally lies along the $-y$ axis is restored to the $+z$ axis such that it is unaffected by G_1. The phases of the remaining ^{1}H pulses in the sequence are adjusted appropriately to maintain the water magnetization aligned along $+z$ at the beginning of the acquisition, thus avoiding saturation effects. The inversion of phase ϕ_5 in subsequent scans is compensated by a concomitant $\pi/2$ shift of ϕ_3.

The dependence of the cross- and diagonal-peak intensities on the homonuclear coupling constant and the duration of the isotropic mixing period τ_m has been analyzed in detail in Ref. (*21*). The (HN)CO(CO)NH scheme contains relatively long periods T in which carbonyl antiphase magnetization with respect to the coupled nitrogen is refocused. Simultaneously, ^{13}C′ in-phase magnetization is partially converted into an antiphase state by the homonuclear scalar interaction prior to the TOCSY mixing period, and both terms contribute to the finally detected signals, introducing $\cos(2\pi J_{C'C'}T)$ factors in the transfer function. Here, a simplified expression can be used, as the evolution of ^{15}N antiphase terms with respect to long-range coupled nitrogens can safely be ignored for the very small coupling constants and the short free precession periods $\Delta = T_N$ during which they are active in the HNNH-TOCSY experiment. Therefore, the cross-peak to diagonal-peak intensity ratio is given by $I_C/I_D = [1 - \cos(2\pi J_{NN}\tau_m)]/[1 + \cos(2\pi J_{NN}\tau_m)]$. However, this expression does not take into account that cross peaks and diagonal peaks detected at $F_2 = \omega(^{15}N_i)$ and $F_3 = \omega(^1H^N_i)$ in general experience different losses up to the start of the ^{15}N mixing period as a result of transverse relaxation, imperfect pulses, and incomplete buildup of equilibrium magnetization. These factors cancel out when the intensities of the diagonal peaks of residues i and $i + 1$ as well as both cross peaks between them are known. In this case the ratio I_C/I_D has to be replaced by $\{[I_{C(i\pm1,i)} \cdot I_{C(i,i\pm1)}]/[I_{D(i\pm1)} \cdot I_{D(i)}]\}^{1/2}$ (*21*). In contrast to ''out-and-back'' type experiments like the HNN, it is therefore mandatory to measure the intensity of four components to obtain accurate results, rendering the method more susceptible to resonance overlap. For this reason we have applied two versions of the HNNH-TOCSY, one with ^{15}N evolution during t_1 (Fig. 1B) and the other with ^{1}H evolution (Fig. 1C).

Each of the two HNNH-TOCSY variants was performed twice using mixing times of 145 and 181 ms, corresponding to four and five cycles of DIPSI-3, respectively. As demonstrated in Fig. 4, the (H)NNH-TOCSY and H(N)NH-TOCSY spectra supplemented each other with respect to the resolution of diagonal and cross peaks. For instance, the cross-peak intensities of residue pairs V 33/D 34 and S 96/S 97 could not be evaluated in the H(N)NH version because of a near-degeneracy of the amide proton chemical shifts, whereas in the (H)NNH version diagonal and cross peaks were well resolved owing to the large difference in the corresponding ^{15}N frequencies. The complementary situation was encountered for C 57/S 58, where the cross peaks could only be identified in the (H)NNH- but not in the H(N)NH-TOCSY spectra. Furthermore, a separate measurement of $^3J_{NN}$ coupling constants for K 87/V 88 and V 88/A 89 was prevented in the H(N)NH-TOCSY because of almost degenerate $^1H^N$ resonance frequencies of K 87 and A 89, whereas the two cross peaks detected for V 88 are separated in the ^{15}N (F_1) dimension of the (H)NNH-TOCSY. In an analogous way the G 92/F 91 and G 92/C 93 signals which exactly coincided in the (H)NNH-TOCSY were resolved in the ^{1}H (F_1) dimension of the H(N)NH-TOCSY.

Analysis of the HNNH-TOCSY spectra resulted in 79 $^3J_{NN}$ coupling constants with lower and upper limits of 0.1 and 0.37 Hz, respectively. The rms pairwise differences within the two (H)NNH or the two H(N)NH data sets as well between the respective average values ranged between 0.02 and 0.03 Hz, indicating that these couplings can be quantitatively determined with reasonable precision despite their very low magnitude. As expected, the sensitivity of the HNNH-TOCSY experiments was higher than that of the HNN experiment. Thus, slightly smaller nitrogen–nitrogen couplings could be detected in the former, although the number of scans per increment was halved. No systematic deviation toward higher or lower coupling constants was recognized, the rms difference between the *J*-values extracted from the two types of experiments amounting to 0.04 Hz. Advantages of the HNN sequence are that for each residue pair the intensity of only one diagonal and one cross peak needs to be evaluated and that ^3J information involving nonprotonated nitrogens (i.e., proline residues) can be obtained.

In this study, a total of 82 $^3J_{NN}$ coupling constants could be measured, a graphical representation of which is given in Fig. 5. The values are correlated with the ψ-angles in the 1.7 Å X-ray structure of flavodoxin in the oxidized state

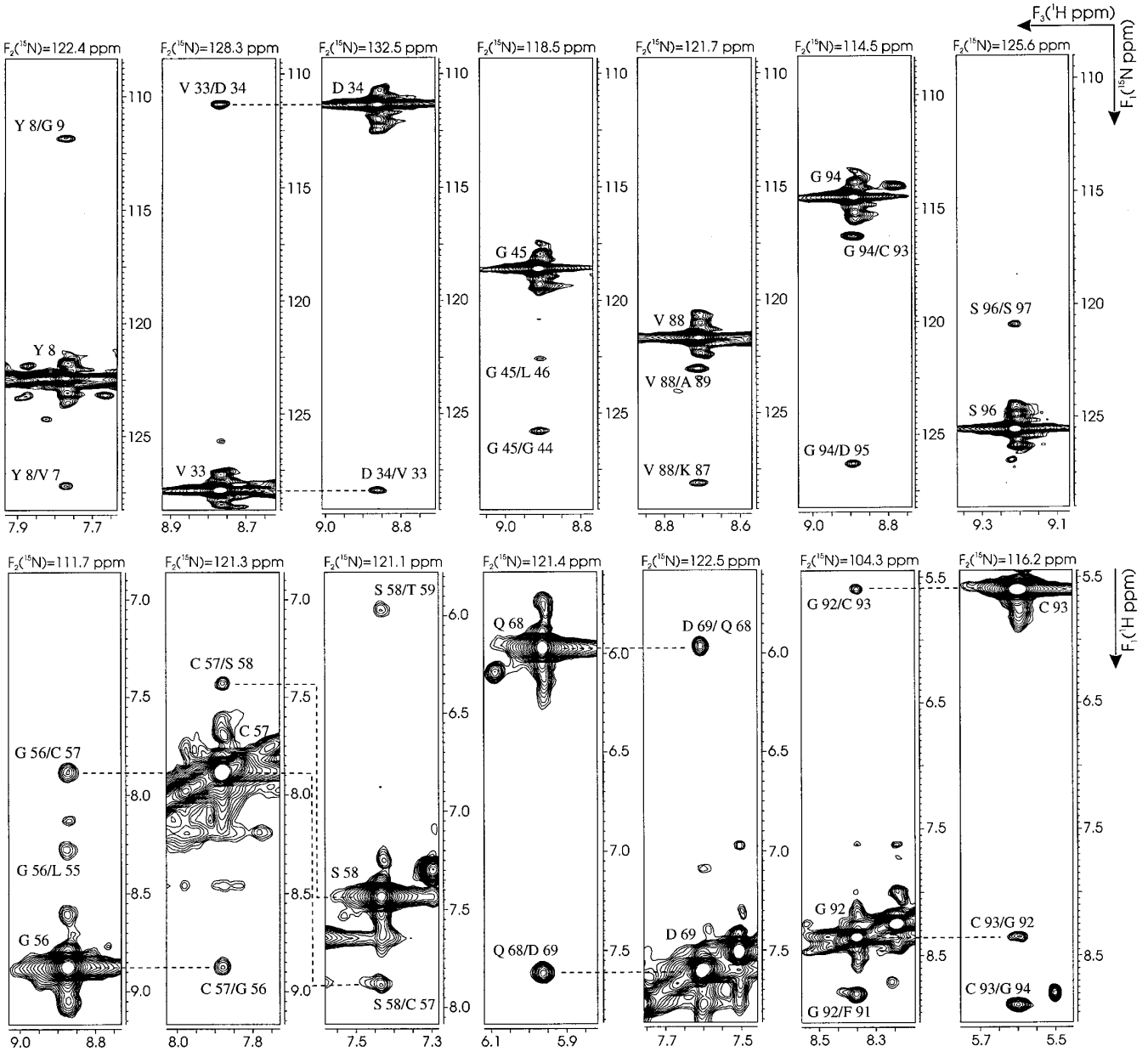

FIG. 4. Application of the HNNH-TOCSY experiment to *D. vulgaris* flavodoxin. The strips are taken from F_1–F_3 planes of the (H)NNH (top) and the H(N)NH (bottom) versions, recorded with mixing times of 181 and 145 ms, respectively. Only positive levels, spaced by a factor of $2^{1/3}$, are drawn. Sequential connectivities between adjacent strips are indicated by dashed lines. Signals belonging to the ^{15}N resonance frequencies of D 34 and of G 44 are folded in the F_1 dimension of the (H)NNH-TOCSY spectrum. The smallest and largest $^3J_{NN}$ coupling constants, respectively, measured for the examples shown are 0.14 Hz (G 45/L 46) and 0.34 Hz (C 93/G 94).

(*35*). Most of the data points are clustered around $\psi = +140°$, typical for β-sheet regions, whereas only relatively few couplings in α-helical residues (ψ around $-40°$) were sufficiently large to give rise to detectable cross peaks, although in flavodoxin the distribution of residues among the two types of secondary structure elements is comparable. It is therefore most likely that the $^3J_{NN}$ scalar interaction follows a Karplus-type relationship with a maximum at $\psi = 180°$ and a second, lower maximum at $\psi = 0°$. Deviations of some data points from the expected behavior may—apart from experimental errors—result from small differences in the backbone geometry between the crystal and the solution state and a varying degree of conformational averaging. As is obvious from Fig. 5, a direct translation of the backbone nitrogen–nitrogen coupling constants into dihedral angles is not conceivable, considering the small variation of the couplings with ψ and the limited sensitivity that can currently be obtained in the quantitative *J*-correlation approach

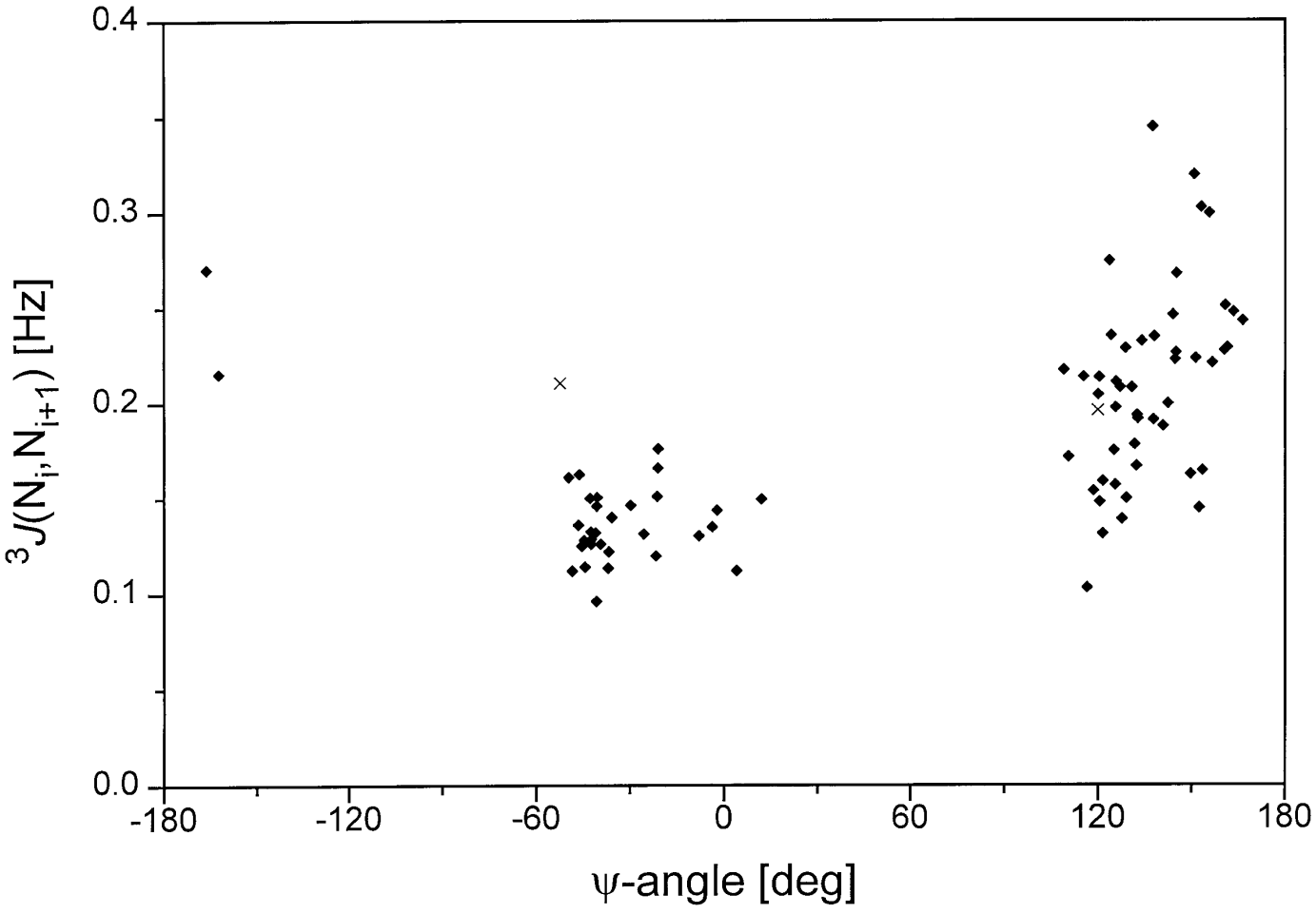

FIG. 5. Correlation between experimental $^3J_{NN}$ coupling constants obtained for oxidized *D. vulgaris* flavodoxin and the corresponding ψ-angles in its crystal structure. The coupling constants represent the average of all measured values available for a particular residue. The sign of the couplings was not determined and is arbitrarily assumed to be uniformly positive. Crosses mark the data points for the two residues of flavodoxin that are sequentially followed by a proline.

presented here. However, coupling constants above 0.2 Hz are indicative of a β-sheet conformation, supplementing the information available from measurements of $^3J(H^{\alpha}_{i},N_{i+1})$. The only exception in the case of flavodoxin was Ile 72 (ψ (X-ray) = $-52°$) for which a $^{15}N-^{15}N$ coupling constant of 0.21 Hz was measured. A possible explanation could be that this interaction, which involves the nitrogen spin of the sequentially following proline residue, is subject to a substituent effect as was found for $^3J(H^{\alpha}_{i},N_{i+1})$ (*10*).

CONCLUSIONS

Simple three-dimensional NMR experiments have been designed which allow scalar $^{15}N-^{15}N$ long-range couplings in proteins to be determined quantitatively, provided that a relatively high concentrated ^{15}N-labeled sample is available and the molecule exhibits favorable relaxation properties. A ψ-angle dependence of the $^3J_{NN}$ couplings is observed which presumably follows a Karplus-type relationship. Their utility in protein structure determinations is, however, restricted to the recognition of conformations with ψ-angles around 180°, where the couplings approach their maximum. In the HNN experiment, two-bond correlations for the guanidino groups in arginine side chains are obtained. It might therefore supplement triple-resonance experiments dedicated for the resonance assignment of these residues (*36–38*).

EXPERIMENTAL

A 4 mM ^{15}N-labeled sample of flavodoxin dissolved in 10 mM potassium phosphate buffer, pH 7.0 was used for all measurements described in this paper. All spectra were recorded at 27°C on a Bruker DMX 600 spectrometer equipped with a pulsed field gradient unit and an actively shielded *xyz*-gradient triple-resonance probe. The HNN experiment was carried out twice with dephasing and rephasing periods δ ($=T_N$) of 120 and 150 ms, using spectral widths of 1625, 1289, and 8993 Hz in F_1, F_2, and F_3, respectively.

The number of complex data points and the corresponding acquisition times in t_1, t_2, and t_3, respectively, were 88 (53.8 ms), 48 (36.5 ms), and 896 (99.7 ms). Accumulation of 16 scans for each FID resulted in measuring times of 111 h for $\delta = 120$ ms and 112 h for $\delta = 150$ ms.

In the HNNH-TOCSY experiments, spectral widths and acquisition times in t_2 and t_3 were identical to those in the HNN. For the (H)NNH version, 94 complex points were recorded in t_1, resulting in an acquisition time of 72.2 ms (SW = 1289 Hz). When amide proton chemical shift evolution was employed, 192 real points were acquired in t_1 without changing the phase of the 90° pulses bracketing the evolution period. The proton carrier was placed at the H_2O frequency (4.75 ppm) such that all detectable resonances were on its low-field side. Using a spectral width of 5.62 ppm (3378 Hz, acquisition time 28.3 ms), signals downfield from 7.56 ppm were aliased into the empty high-field half, but processing the data in the TPPI manner (*39*) shifted the edge of the spectrum by SW/2 such that the apparently unaliased region extended from 4.75 to 10.37 ppm. Addition of eight scans per FID resulted in measuring times between 67 and 68 h for each of the four data sets.

During processing of all spectra, linear prediction was employed to increase the number of t_2 data points to 64. Time-domain data were multiplied by a squared cosine-bell function before Fourier transformation in each dimension.

ACKNOWLEDGMENTS

This work was supported by a grant from the Deutsche Forschungsgemeinschaft (Ru 145/11-2). The help of Prof. Stephen G. Mayhew (University College, Dublin) with the labeling and isolation of the *D. vulgaris* flavodoxin is gratefully acknowledged. We thank Dr. Martin Walsh (EMBL, Hamburg) for making available the refined X-ray coordinates of oxidized flavodoxin and Dr. Jürgen M. Schmidt for providing a program to calculate the effect of differential relaxation on the apparent coupling constants.

Note added in proof. After submission of our manuscript, a pulse sequence similar to the HNNH-TOCSY proposed here has been published by Grzesiek and co-workers (K. Theis, A. J. Dingley, A. Hoffmann, J. G. Omichinski, and S. Grzesiek, *J. Biomol. NMR* **10,** 403 (1997)).

REFERENCES

1. C. Biamonti, C. B. Rios, B. A. Lyons, and G. Montelione, *Adv. Biophys. Chem.* **4,** 51 (1994).
2. A. Bax, G. W. Vuister, S. Grzesiek, F. Delaglio, A. C. Wang, R. Tschudin, and G. Zhu, *Methods Enzymol.* **239,** 79 (1994).
3. D. S. Wishart, and B. D. Sykes, *J. Biomol. NMR* **4,** 171 (1994).
4. B. Reif, M. Hennig, and C. Griesinger, *Science* **276,** 1230 (1997).
5. D. Yang, R. Konrat, and L. E. Kay, *J. Am. Chem. Soc.* **119,** 11,938 (1997).
6. D. M. LeMaster, J. C. Laluppa, and D. M. Kushlan, *J. Biomol. NMR* **4,** 863 (1994).
7. M. Ottiger, and A. Bax, *J. Am. Chem. Soc.* **119,** 8070 (1997).
8. G. T. Montelione, M. E. Winkler, P. Rauenbuehler, and G. Wagner, *J. Magn. Reson.* **82,** 198 (1989).
9. G. Wider, D. Neri, G. Otting, and K. Wüthrich, *J. Magn. Reson.* **85,** 426 (1989).
10. A. C. Wang, and A. Bax, *J. Am. Chem. Soc.* **117,** 1810 (1995).
11. M. Karplus, *J. Chem. Phys.* **30,** 11 (1959).
12. D. B. Davies, and Md. A. Khaled, *J. Chem. Soc. Perkin Trans.* **2,** 187 (1976).
13. D. B. Davies, and Md. A. Khaled, *J. Chem. Soc. Perkin Trans.* **2,** 1327 (1976).
14. N. Juranic, V. Likic, T. Parac, and S. Macura, *J. Chem. Soc. Perkin Trans.* **2,** 1805 (1993).
15. D. B. Davies, Md. A. Khaled, and D. W. Urry, *J. Chem. Soc. Perkin Trans.* **2,** 1294 (1977).
16. F. Delaglio, D. A. Torchia, and A. Bax, *J. Biomol. NMR* **1,** 439 (1991).
17. G. W. Vuister, and A. Bax, *J. Biomol. NMR* **2,** 401 (1992).
18. G. W. Vuister, F. Delaglio, and A. Bax, *J. Biomol. NMR* **3,** 67 (1993).
19. A. S. Edison, F. Weinhold, W. M. Westler, and J. L. Markley, *J. Biomol. NMR* **4,** 543 (1994).
20. J.-S. Hu, and A. Bax, *J. Am. Chem. Soc.* **118,** 8170 (1996).
21. S. Grzesiek, and A. Bax, *J. Biomol. NMR* **9,** 207 (1997).
22. A. J. Shaka, C. J. Lee, and A. Pines, *J. Magn. Reson.* **77,** 274 (1988).
23. A. J. Shaka, P. B. Barker, and R. Freeman, *J. Magn. Reson.* **64,** 547 (1985).
24. D. Marion, M. Ikura, R. Tschudin, and A. Bax, *J. Magn. Reson.* **83,** 393 (1989).
25. A. G. Palmer III, J. Cavanagh, P. E. Wright, and M. Rance, *J. Magn. Reson.* **93,** 151 (1991).
26. L. E. Kay, P. Keifer, and T. Saarinen, *J. Am. Chem. Soc.* **114,** 10,663 (1992).
27. S. Grzesiek, and A. Bax, *J. Am. Chem. Soc.* **115,** 12,593 (1993).
28. L. E. Kay, G. Y. Xu, and T. Yamazaki, *J. Magn. Reson. A* **109,** 129 (1994).
29. G. Otting, B. A. Messerle, and L. P. Soler, *J. Am. Chem. Soc.* **119,** 5425 (1997).
30. A. Bax, D. Max, and D. Zax, *J. Am. Chem. Soc.* **114,** 6923 (1992).
31. A. Hrovat, M. Blümel, F. Löhr, S. G. Mayhew, and H. Rüterjans, *J. Biomol. NMR* **10,** 53 (1997).
32. G. W. Vuister, and A. Bax, *J. Am. Chem. Soc.* **115,** 7772 (1993).
33. T. M. Logan, E. T. Olejniczak, R. X. Xu, and S. W. Fesik, *FEBS Lett.* **313,** 413 (1992).
34. S. Grzesiek, and A. Bax, *J. Biomol. NMR* **3,** 185 (1993).
35. M. Walsh, unpublished results.
36. H. Vis, R. Boelens, M. Mariani, R. Stroop, C. E. Vorgias, K. S. Wilson, and R. Kaptein, *Biochemistry* **33,** 14,858 (1994).
37. T. Yamazaki, S. M. Pascal, A. U. Singer, J. D. Forman-Kay, and L. E. Kay, *J. Am. Chem. Soc.* **117,** 3556 (1995).
38. B. T. Farmer II, and R. A. Venters, *J. Biomol. NMR* **7,** 59 (1996).
39. D. Marion, and K. Wüthrich, *Biochem. Biophys. Res. Commun.* **113,** 967 (1983).